

Dynamics of thin fluid films controlled by thermal fluctuations

S. Nestic^{1,a}, R. Cuerno¹, E. Moro^{1,2}, and L. Kondic³

¹ Departamento de Matemáticas and Grupo Interdisciplinar de Sistemas Complejos (GISC), Universidad Carlos III de Madrid, Avenida de la Universidad 30, 28911 Leganés, Spain

² Instituto de Ingeniería del Conocimiento, Universidad Autónoma de Madrid, 28049 Madrid, Spain

³ Department of Mathematical Sciences, New Jersey Institute of Technology, Newark, New Jersey, USA

Received 30 July 2014 / Received in final form 16 February 2015
Published online 8 April 2015

Abstract. We consider the influence of thermal fluctuations on the dynamics of thin fluid films in two regimes. Working within the stochastic lubrication approximation, we generalize the results on (stochastic) similarity solutions [B. Davidovitch, et al., Phys. Rev. Lett. **95**, 244505 (2005)] that focused on surface tension dominated regime, to gravity-driven relaxation. In particular, we verify numerically the validity of the results in gravity-dominated regime, and find that fluctuations enhance spreading, as in surface tension dominated regime, even in the presence of a faster deterministic relaxation. Considering further the novel case of fluid droplet spreading driven by surface tension and van der Waals forces, our simulations show that the presence of noise affects the value of droplet contact angle.

1 Introduction

Evolution of thin fluid films on substrates is the problem of substantial importance in a number of different fields of science and technology. While there is a huge body of work considering various aspects of this evolution, as outlined in extensive review articles [1, 2], there are only very few works considering the effect of thermal fluctuations [3–6]. These fluctuations are expected to become increasingly more relevant as the thicknesses of the considered films become smaller and may be therefore crucial for understanding the problems involving evolution of films on nanoscale [7].

In the present work, we first discuss in Sect. 2 formulation of a “stochastic lubrication equation” (SLE), where thermal effects are included in the commonly used formulation based on the long-wave asymptotic limit. Scaling properties of this equation are discussed in Sect. 3, where we outline different regimes where the contributions of surface tension, gravity, or noise are expected to be dominant. Then we proceed by discussing the influence of noise in two particular regimes. Section 4 focuses on

^a e-mail: snestic@math.uc3m.es

considering gravity-driven regime, where the effects of wetting (modeled by disjoining pressure) and surface tension are ignored. Section 5 considers a different regime, where the interplay between surface tension, disjoining pressure, and noise governs the evolution. In both regimes we find non-trivial influence of stochasticity on the dynamics. Section 6 is devoted to the summary and brief discussion of future work.

2 Stochastic lubrication equation

In realistic fluid systems the velocity field is not a deterministic function but, rather, a fluctuating one. Hence, it is of interest to consider new effects that can take place when noise is accounted for. The simplest situation corresponds to Gaussian white noise in the stress tensor, as originating from thermal fluctuations in the distribution of molecular velocities [8]. Within linear response theory and considering an incompressible fluid of viscosity η and density ρ , the Navier-Stokes equations read [3–5]

$$\nabla \cdot \mathbf{v} = 0, \quad (1)$$

$$\rho \frac{\partial \mathbf{v}}{\partial t} + \rho(\mathbf{v} \cdot \nabla) \mathbf{v} = \eta \Delta \mathbf{v} - \nabla(p - \Pi) + \nabla \cdot \mathbf{S} + \rho \mathbf{g}, \quad (2)$$

where \mathbf{S} is a symmetric, zero-mean, delta-correlated fluctuation tensor [8]. In Eq. (2) we have allowed for a gravity body force and we have also introduced the disjoining pressure Π , which accounts for the liquid-solid interaction. Macroscopically, the disjoining pressure corresponds to a change in free energy due to the introduction of a surface, as compared with that of the fluid bulk [9]. Microscopically, it originates from the interaction between substrate and fluid molecules, e.g. via van der Waals forces, and becomes particularly important for thin films.

In the present work, we assume that the fluid film thickness, $h = h(x, t)$, where x is the in-plane coordinate, and also assume that $\Pi = \Pi(h)$. We do not include the effects of phase change and assume no-slip boundary condition at the fluid-solid interface. The upper surface of the film remains free. In such a case, the long-wave (lubrification) approximation leads to [4, 5]

$$\eta \partial_t h = \partial_x \left\{ \frac{h^3}{3} \partial_x [-\gamma \partial_x^2 h - \Pi(h) + \rho g h] + \int_0^h dy \int_0^y dy' S(x, y', t) \right\}, \quad (3)$$

where $S = \mathbf{S}_{xy}$ is the only component of the fluctuating stress tensor that appears at lowest non-trivial order in the long-wave expansion. As usual [1], the first three terms inside the brackets on the right-hand-side (RHS) of Eq. (3) represent the surface tension, the disjoining pressure, and the gravity force, respectively. Note that, due to the delta-correlations in the fluctuating stress tensor, the variance of the noise term in Eq. (3) reads

$$\int_0^h dy \int_0^h dy' \int_0^y dy_1 \int_0^{y'} dy_2 \langle S(x, y_1, t) S(x', y_2, t') \rangle = \frac{\eta k_B T}{3} h^3 \delta(x - x') \delta(t - t'), \quad (4)$$

so that the stochastic lubrication equation (SLE) can be finally written as

$$\eta \partial_t h = \partial_x \left\{ \frac{h^3}{3} \partial_x [-\gamma \partial_x^2 h - \Pi(h) + \rho g h] + \sigma h^{3/2} \epsilon(x, t) \right\}, \quad (5)$$

where $\sigma = \sqrt{\eta k_B T / 3}$ and $\epsilon(x, t)$ is a Gaussian white noise with unit variance. For $\sigma = 0$, the well-known deterministic thin film equation is retrieved. We note that there

are other ways to derive Eq. (5). For instance, by linearizing the deterministic thin film equation and using the fluctuation-dissipation theorem, one is led to the same noise term as in Eq. (5) [3]. Likewise, a detailed Fokker-Planck analysis of Eq. (3) leads to the conclusion that it describes the same stochastic process as Eq. (5) [4,5]. Finally, note that Eq. (5) shows the full dimensional dependence on physical parameters. Particular instances of this equation are studied in detail in the following sections. Numerical simulations will be performed in appropriate dimensionless units, that will be specified in each particular case. See the Appendix for some particular examples of correspondence between the dimensionless and physical parameters relevant to particular experiments.

3 Scaling properties of the SLE equation

Spreading of fluid droplets is often considered to be driven by surface tension and gravity forces, represented in the SLE model by the first and third terms inside the brackets on the RHS of Eq. (5). If partial wetting (non-zero contact angle) is to be considered, one possibility is to include in the model the disjoining pressure that results from the balance between attractive and repulsive contributions to the interface potential induced by van der Waals interactions. Such an approach allows to describe accurately film break-up and droplet formation through the occurrence of morphological instabilities under e.g. dewetting conditions [10]. The disjoining pressure stops droplet spreading or contraction and sets a fixed macroscopic contact angle. We will consider such a process in Sect. 5. In the present section, we will focus on spreading of completely wetting droplets (zero contact angle), therefore the disjoining pressure will be omitted.

As it is well known, the spontaneous spreading of a fluid droplet under the action of deterministic forces leads to power-law scaling of a typical length-scale, like e.g. the droplet width ℓ , as $\ell(t) \sim t^n$. This is the content of Tanner's law [11,12], where the value of the exponent n depends on the specific relaxation term which is assumed, e.g. $n = 1/7$ for surface-tension-dominated flow. Mathematically, this property is related to the existence of similarity solutions to the corresponding thin film equation [13]. Using a self-similar argument for the SLE, in [3] stochastic fluctuations were shown to modify the spreading exponent value to $n = 1/4$ for surface-tension driven flow. Here, our goal is to generalize the arguments in [3] for a more general SLE of the form given by Eq. (5), neglecting (for now) disjoining pressure contribution.

Inspired by the success of scaling analysis to describe the long-time behavior of non-equilibrium interfaces in the presence of fluctuations [14], in [3] the effect of a rescaling of coordinates and fields in the SLE with surface tension only, was considered. In particular, in that work the behavior under the change of variables

$$x = b\tilde{x} \quad t = b^z\tilde{t} \quad h = b^\alpha\tilde{h}, \quad (6)$$

where $b > 1$ is an arbitrary factor and α and z are constants that remain to be fixed, was considered. In the more general case considered here, the various terms on the RHS of Eq. (5) scale differently under this operation. In the rescaled coordinates and dropping the tildes, the ensuing SLE takes on the exact same form as Eq. (5), but with modified parameters

$$\widetilde{\gamma/\eta} = (\gamma/\eta)b^{z+3\alpha-4}, \quad \widetilde{\rho g/\eta} = (\rho g/\eta)b^{z+3\alpha-2}, \quad \widetilde{\sigma/\eta} = (\sigma/\eta)b^{(z-3+\alpha)/2}. \quad (7)$$

Conservation of fluid volume, $V(t) = \int h(x,t)dx$, requires $\alpha = -1$, independently of the physical forces considered. The remaining coefficient, z , can be obtained by

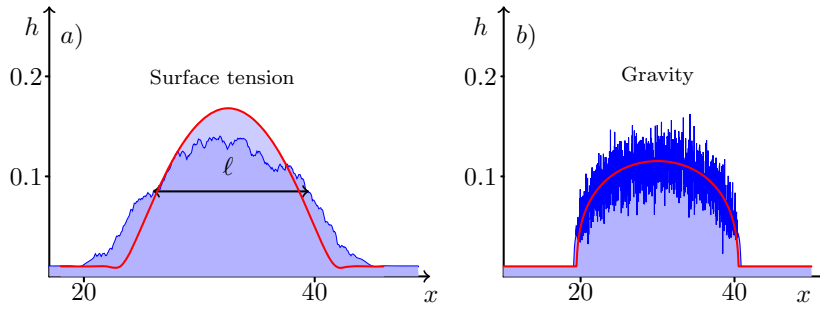


Fig. 1. Deterministic and stochastic droplets in the surface-tension (a) and gravity (b) dominated flows, starting from the same initial condition. In both cases the thick red solid line corresponds to the deterministic solution, while the thin blue line corresponds to a single realization of a droplet, as described by the corresponding SLE. In both cases fluctuations speed up spreading, the effect being larger in the surface tension dominated system. Note the different scales employed for the horizontal x and vertical h axes.

requesting that the rescaled SLE remains unchanged, thereby imposing statistical self-invariance [14], namely, the dynamics and fluctuations of the rescaled height field $\tilde{h}(x, t) = b^{-\alpha}h(bx, b^z t)$ will be indistinguishable from those of $h(x, t)$ [15]. In principle, such an invariance can strictly hold only if a single term occurs in the equation, leading to $z = 7, 5, 4$ if that term is due to surface tension, gravity, or the noise contribution, respectively. If two terms occur simultaneously, e.g. surface tension and noise, as studied in [3–5], Eq. (7) provides expectations on the relevance of each term during the system evolution. Thus, $z = 7$ as dictated by surface tension implies $\tilde{\sigma} > \sigma$, suggesting that stochastic fluctuations will become more and more relevant at increasing time and length scales. We note in passing that this scaling argument can be generalized and applied for any deterministic relaxation term in the SLE whose linearized form is proportional to $\partial_x^m h$ for any $m > 1$; it can be easily checked that the corresponding rescaled parameter grows as b^{z-3-m} , to be compared with b^{z-4} for the noise.

Consider now a spreading problem, such that a droplet of initial width $\ell(t = 0)$ evolves under Eq. (5). Statistical self-similarity under Eq. (6) implies that, if we rescale time by a factor c , the system configuration only remains statistically invariant provided length scales are rescaled by a factor $c^{1/z}$. Hence, $\ell(t) \sim t^{1/z}$. Indeed, when surface tension dominates, we obtain the well-known Tanner’s law [11], where $\ell(t) \sim t^{1/7}$. However, as noted above, there is a long-time regime $t \gg 1$ such that noise fluctuations dominate over the deterministic relaxation. In that regime we find that $\ell \sim t^{1/4}$, implying much faster spreading due to thermal fluctuations. This result was explicitly confirmed numerically in [3] by simulating the corresponding SLE, Eq. (5) without gravity and disjoining pressure. Figure 1a shows a comparison between droplet spreading by surface tension only, and if thermal fluctuations are additionally considered. The simulations have been carried out as in [3], in dimensionless units for which the height of the initial droplet is unity.

4 Influence of fluctuations on gravity-driven droplet spreading

The discussion from the preceding section leads one to expect a droplet spreading law of the type $\ell \sim t^{1/5}$ when the process is induced by gravity alone. Note that this is a faster spreading rate than Tanner’s law for surface-tension driven flow. In turn, if we allow for thermal fluctuations, we still expect noise to dominate the long-time

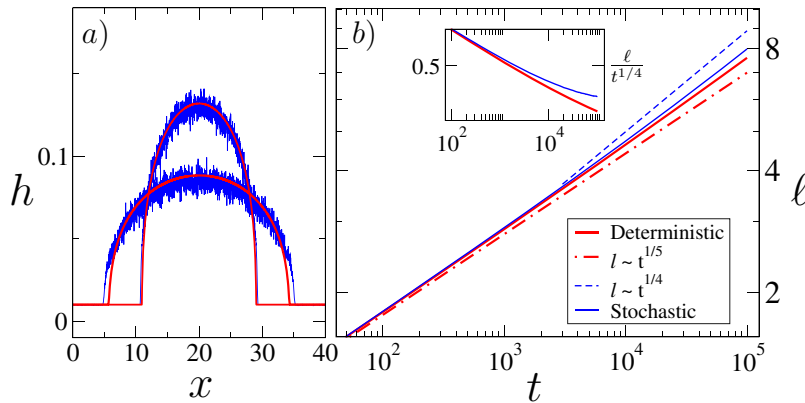


Fig. 2. (a) Deterministic (thick red line) and stochastic (thin blue line; averaged over 15 stochastic realizations) droplets relaxing under gravity from the same initial condition, at times $t = 10^4$ and $8 \cdot 10^4$, top to bottom. (b) Droplet width vs time for the deterministic and stochastic simulations. The dot-dashed (dashed) line indicates the deterministic (stochastic) spreading law, as in the legend. The inset plots a rescaled droplet width in order to compare with the noise-dominated behavior.

evolution, where the spreading law crosses to the $\ell \sim t^{1/4}$ behavior. With respect to specific situations in which such type of crossover dynamics might be observed, a natural context could be ultralow surface tension fluids, such as suitable colloid-polymer mixtures [16, 17].

In this section we explicitly test the scaling hypothesis in such a gravity-dominated regime, in order to confirm that fluctuations change the spreading law in an observable manner. Working as above in dimensionless units in which the height of the initial droplet is unity (see Appendix), the SLE we thus consider is

$$\partial_t h = \partial_x \left\{ h^3 \partial_x h + \sigma h^{3/2} \epsilon(x, t) \right\}. \quad (8)$$

We employ the same kind of algorithm that was used to simulate droplet spreading driven by surface tension and noise in [3], see the Appendix. Unless otherwise stated, we have considered $\sigma = 0$ ($10^{-5/2}$) for the deterministic (stochastic) simulations.

Figure 1b illustrates the evolution of an initial droplet as in Fig. 1a, but as described by Eq. (8). Note that, since the smoothening effect of surface tension is not present, it would not be surprising to observe shock-like spreading of the drop front. Nevertheless, slopes in Fig. 1b are not as high as suggested by naked-eye inspection, note the difference in horizontal and vertical scales. On the other hand, given that the expected spreading laws due to gravity and fluctuations are relatively similar, and in order to appreciate the expected crossover, we have used a relatively large value of σ compared to the height of the precursor film, $h_* = 0.01$. Numerical results indeed indicate somewhat faster spreading for the stochastic droplets than for their deterministic counterparts, see Fig. 2a. Here, we show the deterministic and the stochastic evolutions at two different times. Indeed, one can appreciate an enhancement of the droplet width in the latter case.

In order to gain more quantitative understanding, we measure the average rate by which the characteristic width of the droplets, ℓ , evolves. To estimate it, we again follow [3] and consider the averaged second moment of the height profile,

$$\ell(t) = \left\langle \left[\frac{1}{V} \int dx (x - X)^2 h(x, t) \right]^{1/2} \right\rangle, \quad (9)$$

where $X = [\int dx x h(x, t)]/V$ is the instantaneous position of the droplet center, V as above is the total droplet volume, which remains constant in time, and $\langle \dots \rangle$ represents an average over realizations of the noise $\epsilon(x, t)$. As we can see in Fig. 2b the stochastic system departs from the deterministic behavior for $t \gtrsim 3000$, crossing over towards the purely noise-dominated regime. Notice that, due to the necessarily large value of the precursor thickness, which becomes comparable to the droplet height for long enough times, even the deterministic spreading yields the spreading exponent slightly larger than the $1/5$ expected value. In any case, there is a small but significant difference in droplet width between the deterministic and the stochastic cases, purely noise-dominated spreading being expected for sufficiently long times. As noted in the Appendix, appropriate polymer-colloid mixtures exist [16, 17] which are characterized by very small (ultralow) values of the surface tension $\gamma \lesssim 1 \mu\text{N/m}$ and capillary length ($\simeq 10 \mu\text{m}$). This implies thermal fluctuations with a strength which is comparable to the noise amplitude we have employed in our present simulations. Thus, they constitute potential experimental contexts in which gravity-driven spreading may be indeed enhanced by thermal noise.

5 Influence of fluctuations on the contact angle

We now switch to a related situation encompassed by the SLE, Eq. (5), in which thermal fluctuations again can be seen to have non-negligible effects. Consider a spreading drop whose evolution is governed by surface tension and ignore gravity. Furthermore, consider the drop to be partially wetting with non-zero contact angle, θ , determined by disjoining pressure. In this section we will discuss whether and how the presence of fluctuations influences the value of θ . One motivation for this discussion is that there are often substantial differences between the predictions of deterministic theory and experimentally measured contact angles, see e.g., [18] and the references therein. It is natural to consider whether these differences may be due to the neglect of thermal noise in the deterministic theory. In the deterministic system, a well-defined contact angle between the fluid droplet and the substrate arises as an interplay between surface tension and van der Waals forces [10, 12]. The specific form of the disjoining pressure depends on the material properties, and a variety of functional forms and parameters have been used. Here, we consider commonly used power-law form [12], $\Pi(h) \approx 1/h^n - 1/h^m$ with $(n, m) = (3, 2)$. Hence, we consider the following SLE

$$\partial_t h = \partial_x \left\{ h^3 \partial_x \left[-\partial_x^2 h + \frac{A}{h^2} - \frac{B}{h^3} \right] + \sigma h^{3/2} \epsilon(x, t) \right\}, \quad (10)$$

where A and B are material-dependent constants and units have been rescaled so as to have an initial droplet of unit height, see Appendix. The choice $B = Ah_*$ leads to the equilibrium film (also called the precursor film) of thickness h_* . The constant A is proportional to the Hamaker constant that characterizes vdW interactions [9] and is functionally related to the value of θ under the corresponding wetting conditions. The specific question we address here is how this relation is modified when fluctuations are taken into account.

To answer this question, we have simulated droplet spreading as described by the SLE, Eq. (10), and its deterministic limit, employing the same numerical algorithm as in the previous section (see the Appendix) with surface tension term treated implicitly and van der Waals interactions and fluctuations explicitly. We use $h_* = 0.05$ and $\sigma = 0$ ($10^{-3/2}$) for the deterministic (stochastic) simulations, respectively. Special care has been taken in obtaining average shapes in the latter, taking into account

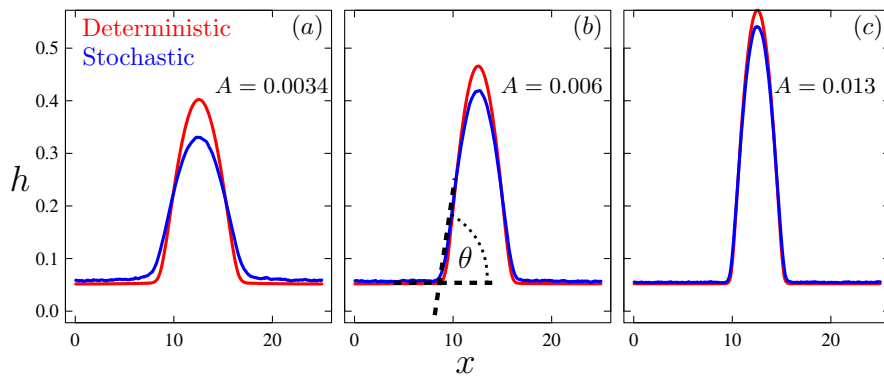


Fig. 3. Deterministic and stochastic droplet spreading from numerical simulations of Eq. (10) at the stationary state. The stochastic shapes have been averaged over 100 noise realizations. Panels (a) through (c) correspond to increasing values of A , as given.

that fluctuations can induce droplet motion. The idea is to calculate the droplet center of mass X as defined above, and then average droplets over noise realizations, provided all of them have been centered around this point.

Figure 3 shows the droplet shapes at times at which spreading has stopped and time-independent value of the contact angle can be extracted. The results show that on average, θ [defined as in Fig. 3b] for a stochastic droplet is smaller than the deterministic one for the same system constants γ and A . For instance, in Fig. 3a fluctuations decrease θ from 6° in the deterministic case to 4° in the stochastic system. Note that small-angle approximations to $A(\theta)$ [10] predict 15° for the deterministic case. Furthermore, Fig. 3 shows that the difference between the deterministic and the stochastic shapes increases for decreasing A , with the value of θ found for stochastic simulations being consistently smaller than in deterministic ones. Fluctuations also induce an increase in the effective value of the equilibrium film, h_* . As a consequence, there is a sizeable reduction in the droplet height due to volume conservation.

Figure 4 gives more detailed information about the influence of noise on droplet spreading. In panel (a), the deterministic and stochastic time evolutions of $\ell(t)$ are shown for different values of A . As in Fig. 3, larger stationary ℓ values are found for smaller values of the Hamaker constant, stochastic films being consistently wider than their deterministic counterparts, see also Fig. 4b. The systematic increase of ℓ at steady-state with the noise amplitude σ is shown in Fig. 4c.

6 Conclusions and outlook

In the present paper we have considered the influence of thermal fluctuations on dynamics of spreading drops in two regimes: (i) gravity-dominated regime, where capillary effects have been ignored, and (ii) surface tension-dominated regime for spreading of partially wetting drop, where contact angle is introduced by disjoining pressure. In both cases we find that stochastic effects influence the dynamics, leading to faster spreading for the gravity-dominated regime, and decreasing the (deterministic) contact angle. For the former case, we corroborate the asymptotic large effect on the fluctuations found in [3] even for negligible surface tension, suggesting that spreading at large stages is always dominated by noise fluctuations. In the latter case the effect of contact angle decrease is particularly obvious for a decreasing value of Hamaker constant, suggesting a non-trivial effect whose relevance for realistic systems remains to be assessed.

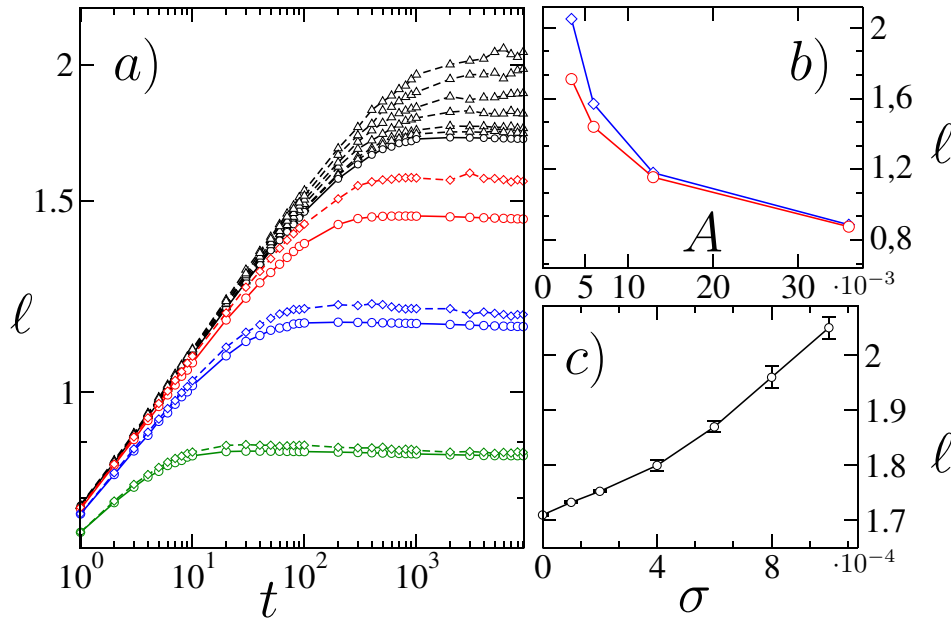


Fig. 4. (a) Droplet width vs time for $A = 0.036, 0.013, 0.006$, and 0.0034 , bottom to top. Deterministic values (circles, solid lines) remain systematically below the average stochastic values (diamonds and triangles, dashed lines). Stochastic simulations have been averaged over 100 noise realizations. The $A = 0.0034$ case (triangles, black dashed lines) was simulated for noise strengths $\sigma = 0.0001, 0.0002, 0.0004, 0.0006, 0.0008, 0.001$ (bottom to top), higher ℓ values being obtained for higher σ . (b) Droplet width vs. Hamaker constant for the deterministic (circles) and stochastic (diamonds) systems, for $\sigma = 0.001$. Statistical errors are smaller than the symbol sizes. (c) Droplet width vs noise strength σ for $A = 0.0034$. In all panels lines are guides to the eye.

Inclusion of stochastic contribution together with disjoining pressure term in the governing stochastic lubrication equation now allows for considering a number of open problems, including quantifying the influence of noise on film breakup, dewetting and pattern formation for fluid films of thickness on nanoscale. Computational investigation of these problems, based on fully nonlinear formulation, is currently in process.

Partial support for this work has been provided by MINECO (Spain) grants No. FIS2010-22047-C05-04 (S. N. and E. M.) and No. FIS2012-38866-C05-01 (R. C.), and by NSF grant No. CBET-1235710 (L. K.). S. N. acknowledges additional support by Universidad Carlos III de Madrid.

Appendix A: Numerical methods and physical scales

The algorithm used in the numerical simulations of Eq. (5) is based on the standard implicit (Crank-Nicholson) discretization [13], where the high-order spatial derivatives are treated implicitly, while the van der Waals and noise terms are treated explicitly. In the simulations discussed in Sect. 4, a regularizing precursor layer of thickness $h_* = 0.01$ has been introduced in order to avoid issues related with the loss of positivity.

For the spreading problem in the gravity-dominated regime, Eq. (8) has been written in dimensionless units in which $\hat{h} = h/h_c$, $\hat{x} = x/h_c$, and $\hat{t} = t/t_c$, so that

$t_c = 3\eta/(\rho gh_c)$, $\hat{\sigma} = (k_B T/\rho gh_c^4)^{1/2}$, hats have been disposed of, and h_c equals the thickness of the initial droplet. For example, in the colloid-polymer mixtures studied in [16,17], one has $\rho g \simeq \gamma/h_c^2$, where $\gamma \lesssim 1 \mu\text{N/m}$ and $h_c \simeq 10 \mu\text{m}$. Hence, at room temperature $T = 300 \text{ K}$, the dimensionless noise amplitude is $\hat{\sigma} \simeq 0.05$, even slightly larger than the value employed in our simulations. We have moreover used space and time steps $\delta x = \delta t = 0.01$, respectively, and a one-dimensional system size $L = 4000$. We have implemented no-flux boundary conditions along the x axis. The region where fluctuations dominate the spreading process is where they are comparable to the droplet height. Contrary to the surface-tension-dominated regime, the low orders of spatial derivatives in the gravity-dominated regime fluctuations induce large (unphysical) fluctuations in the precursor layer. In order to avoid non-positivity issues, we switch off the noise at positions where the droplet height is less than half its value at the center.

With respect to the stochastic contact angle, Sect. 5, Eq. (10) corresponds to dimensionless units [3] in which $\hat{h} = h/h_c$, $\hat{x} = x/h_c$, and $\hat{t} = t/t_c$, so that $t_c = 3\eta h_c/\gamma$, $\hat{\sigma} = (k_B T/\gamma h_c^2)^{1/2}$, hats have been disposed of, and again h_c equals the thickness of the initial droplet. A typical system that could be translated to our non-dimensional description would be the liquid metal thin films considered in [18], where $\gamma = 1.3 \text{ N/m}$, $T = 2000 \text{ K}$, and $h_c \in [5, 15] \text{ nm}$, so that $\hat{\sigma} \in [10^{-2}, 3 \cdot 10^{-2}]$. Also a noise strength $\hat{\sigma} = 10^{-3/2}$ is comparable to the temperatures, $50 - 60 \text{ }^\circ\text{C}$, that were used in [4,5] for polymer films. We note that in general the value of the surface tension can depend non-trivially on temperature. Here, in order to unambiguously identify the influence on the dynamics of thermal noise in the distribution of molecular velocities, we approximate γ by a temperature-independent value. In our simulations, we have further used $h_* = 0.05$, $\delta x = 0.05$, $\delta t = 0.01$, system size $L = 500$, and again no-flux boundary conditions.

References

1. A. Oron, S.H. Davis, S.G. Bankoff, *Rev. Mod. Phys.* **69**, 931 (1997)
2. R.V. Craster, O.K. Matar, *Rev. Mod. Phys.* **81**, 1131 (2009)
3. B. Davidovitch, E. Moro, H. Stone, *Phys. Rev. Lett.* **95**, 244505 (2005)
4. G. Grun, K. Mecke, M. Rauscher, *J. Stat. Phys.* **122**, 1261 (2006)
5. S.K. Mecke, M. Rauscher, *J. Phys. Condens. Matter* **17**, S3515 (2005)
6. T.D. Nguyen, M. Fuentes-Cabrera, J.D. Fowlkes, P.D. Rack, *Phys. Rev. E* **89**, 032403 (2014)
7. L. Bocquet, E. Charlaix, *Chem. Soc. Rev.* **39**, 1073 (2010)
8. L.D. Landau, E.M. Lifshitz, L.P. Pitaevskii, *Statistical Physics*, Part 2 (Pergamon Press, Oxford, 1980)
9. H.-J. Butt, K. Graf, M. Kappl, *Physics and Chemistry of Interfaces* (Wiley-VCH, Weinheim, 2003)
10. J.A. Diez, L. Kondic, *Phys. Fluids* **19**, 072107 (2007)
11. L. Tanner, *J. Phys. D* **95**, 1473 (1979)
12. D. Bonn, J. Eggers, J. Indekeu, J. Meunier, E. Rolley, *Rev. Mod. Phys.* **81**, 0034 (2009)
13. J.A. Diez, L. Kondic, A. Bertozzi, *Phys. Rev. E* **63**, 011208 (2000)
14. A.-L. Barabási, H.E. Stanley, *Fractal Concepts in Interface Growth* (Cambridge University Press, Cambridge, UK, 1995)
15. M. Kardar, *Statistical Physics of Fields* (Cambridge University Press, Cambridge, UK, 2007)
16. D.G. Aarts, M. Schmidt, H.N. Lekkerkerker, *Science* **304**, 847 (2004)
17. Y. Hennequin, D. Aarts, J. van der Wiel, G. Wegdam, J. Eggers, H. Lekkerkerker, *D. Bonn, Phys. Rev. Lett.* **97**, 244502 (2006)
18. A.G. González, J.A. Diez, Y. Wu, J.D. Fowlkes, P.D. Rack, L. Kondic, *Langmuir* **29**, 2378 (2013)